Reactions Between Dimanganese, Dirhenium, and Manganese–Rhenium Decacarbonyl and Oxidants

STEVEN P. SCHMIDT, FRED BASOLO*,
Chemistry Department, Northwestern University, Evanston, Ill. 60201, U.S.A.
and WILLIAM C. TROGLER*
Department of Chemistry, D-006, University of California at San Diego, La Jolla, Calif. 92093, U.S.A.

(Received September 25, 1986)

Abstract

The dimetal decacarbonyls $M_2(CO)_{10}$, where M_2 = Mn_2, MnRe, and Re_2, do not react with anionic strong oxidants such as $Fe(CN)_6^{3-}$ or $IrCl_6^{2-}$ in CH_3CN solvent nor with neutral or cationic weak oxidants. Strong cationic oxidants such as NO^+, $Fe(phen)_3^{3+}$, and Cu^{2+} rapidly oxidize $M_2(CO)_{10}$ to $2M(CO)_5(NCCH_3)^+$ in acetonitrile solvent. The kinetics for the reaction suggest it proceeds according to a bimolecular outer sphere mechanism.

Introduction

Redox reactions of metal carbonyl clusters form an important class of reactions, yet there have been few kinetic studies of the mechanism of the electron transfer process [1]. Metal clusters, including carbonyl clusters, are ideal for such studies because of their chemical stability and varied oxidation states. For example, Ferguson and Meyer [2] studied $[CpFe(CO)]_4$ ($Cp = C_5H_5$), where four electrochemically reversible redox states (+2, +1, 0, −1) were found. The monocation, $[CpFe(CO)]_4^+$, was isolated as the hexafluorophosphate salt. The dication was observed as a transient species by cyclic voltammetry.

Early work on the kinetics of cluster electron transfer mechanisms was reported by Espenson [3–5] for hexanuclear tantalum halides. Several metal ion oxidants, generally used as perchlorate salts, react with $[Ta_6Cl_{12}]^{2+}$ to form $[Ta_6Cl_{12}]^{3+}$. The rate law is second order, being first order in both oxidant and cluster (eqn. (1)).

$$[Ta_6Cl_{12}]^{2+} + Ox \xrightarrow[HClO_4]{25\ °C} [Ta_6Cl_{12}]^{3+} + Red \qquad (1)$$

Ox = Hg^{2+}, Ce^{4+}, Cu^{2+}, $HCrO_4^-$, *cis*-$[Co(NH_3)_4(H_2O)Cl]^{2+}$

*Authors to whom correspondence should be addressed.

Braddock and Meyer [6] reported an important example of the two-electron oxidation of $[CpFe(CO)_2]_2$ with the oxidants $[CpFe(CO)]_4^+$ and $[Ru(bipy)_2Cl_2]^+$ (bipy = 2,2′-bipyridyl) in CH_3CN solvent (eqn. (2)).

$$[CpFe(CO)_2]_2 + 2Ox + 2CH_3CN \longrightarrow 2[CpFe(CO)_2(NCCH_3)]^+ + 2Red \qquad (2)$$

The rate law was found to be similar to the previous example. It was proposed that transfer of a single electron from the iron dimer to the oxidant limits the rate. The electron is probably removed from the metal–metal bond yielding the intermediate $[CpFe(CO_2)]_2^+$, which reacts with oxidant and solvent to yield $CpFe(CO)_2(CH_3CN)^+$.

Connelly and Dahl [7] examined reactions of the nitrosonium cation with transition metal complexes. In acetonitrile the reaction between $M_2(CO)_{10}$ (M_2 = Mn_2, Re_2) compounds and two equivalents of $NOPF_6$ yields $[M(CO)_5(NCCH_3)]^+$ (eqn. (3)).

$$M_2(CO)_{10} + 2NOPF_6 \xrightarrow[CH_3CN]{25\ °C} 2[M(CO)_5(NCCH_3)]PF_6 + 2NO \qquad (3)$$

M_2 = Mn_2, Re_2

It was reported [8] that reaction occurs immediately on mixing. The nitrosonium ion reacts with other organometallics in acetonitrile, or in methanol/toluene mixtures, to produce cationic nitrosyls, hydrides, and nitriles, as well as products of one-electron oxidation [9]. A study [10] of the oxidative homolytic cleavage of $Mn_2(CO)_{10}$ by TCNE reports an EPR spectrum that consists of the spectra of the TCNE radical anion and another species (eqns. (4) and (5)).

0020-1693/87/$3.50

$$Mn_2(CO)_{10} + TCNE \xrightarrow{slow} [Mn_2(CO)_{10}]^+ + TCNE^{\cdot -} \quad (4)$$

$$[Mn_2(CO)_{10}]^+ \xrightarrow[fast]{solv} Mn(CO)_5^{\cdot} + [Mn(CO)_5(solv)]^+ \quad (5)$$

This suggests a one-electron transfer from $Mn_2(CO)_{10}$ to TCNE. The same reaction does not occur with $Re_2(CO)_{10}$.

Previously, we characterized [11] the mechanism of halogenation of $Mn_2(CO)_{10}$, $Re_2(CO)_{10}$, and $MnRe(CO)_{10}$. This reaction (e.g. eqn. (6)) proceeds by an inner sphere [12] oxidation

$$Mn_2(CO)_{10} + 2I_2 \xrightarrow{CH_3CN} Mn(CO)_5I + [Mn(CO)_5(NCCH_3)]I_3 \quad (6)$$

mechanism where one end of the halogen attacks the metal–metal bond to produce a bridged intermediate. An inner sphere process has also been established [13] for the reduction of $Os_6(CO)_{18}$ by I^-. It would be informative to define outer sphere mechanisms of these clusters for comparative purposes. Kinetic studies of the oxidation of $M_2(CO)_{10}$ ($Mn_2 = Mn_2$, Re_2, MnRe) by NO^+ and Cu^{2+} will be described as well as reactions with other 1 and 2-electron oxidants.

Experimental

Materials

Diethyl ether was dried over sodium benzophenone ketyl and distilled before use. Acetonitrile (Burdick and Jackson, 0.01% H_2O) was purified by three successive distillations under nitrogen, the first from CaH_2 and those following from P_2O_5 (~5 g/liter). Carbon tetrachloride, methylene chloride, and ethanol were reagent grade. Dimanganese decacarbonyl, purified by sublimation at 60 °C and 0.1 mm Hg, and dirhenium decacarbonyl were obtained from Strem Chemicals. Nitrosonium tetrafluoroborate (Alfa) was purified [14] by slow heating to 185 °C at 0.1 mm vacuum to sublime it onto a dry ice/acetone cold finger. Triphenylphosphine (Aldrich) was recrystallized from ethanol. $[NH_4]_2[Ce(NO_3)_6]$ (Smith), $Tl(O_2CCF_3)_3$ (Pfaltz and Bauer), $Na_2[IrCl_6]\cdot 6H_2O$ (Alfa), TCNE (Aldrich), $[n\text{-}Bu_4N][BF_4]$ (Aldrich), $[Et_4N][Cl]$ (Eastman), [PPN][Cl] (Aldrich), $AgCF_3SO_3$ (Aldrich), $K_3[Fe(CN)_6]$ (Baker), $FeCl_3\cdot 6H_2O$ (Mallinckrodt), $CuCl_2\cdot 2H_2O$ (Baker), $AgBF_4$ (Alfa), and basic copper carbonate (Baker) were used without purification.

Spectral Studies and Kinetic Methods

IR spectra were recorded in 0.1 mm or 0.2 mm CaF_2 cells with a Perkin-Elmer 283 or a Nicolet 7199 FTIR spectrometer. Electronic spectra were recorded in 1.00 cm quartz cells, adapted for use with air-sensitive solutions, with a Perkin-Elmer 330 or Hitatchi 320 spectrometer. The stopped-flow spectrometer was an Applied Photophysics (London) Model 1705 instrument equipped with a Tektronix 564 storage oscilloscope for data reduction. Drive syringes were modified for work with air-sensitive solutions, by fitting Hamilton Model 1005 5 ml gas tight syringes with Teflon nose cones and metal fittings constructed by the Northwestern University Physics Shop. Storage reservoirs for reactants were Hamilton Model 1030 30 mL gas tight syringes or specially constructed Schlenk funnels attached to the valve block through Hamilton micro-valves. Reservoirs were placed above the value block for gravity assist when filling drive syringes. The reactant reservoirs were attached directly to a vacuum line for air-sensitive manipulations. All exposed syringe surfaces were lined with foil for protection from light. The drive syringes, valve block, and mixing chamber were thermostatted (±0.2 °C) by a model RTE-8 Neslab refrigerated circulating bath.

For reactions with $NOBF_4$ the maximum absorbance changes in the UV spectrum occurred at the position of the σ–σ^* transition of the decacarbonyls. Kinetics measurements were carried out under pseudo-first order conditions with at least a 50-fold excess of $NOBF_4$. Solutions of reactants were prepared by weighing solid samples in the dry box and adding CH_3CN solvent. Observed rate constants were calculated by determining absorbances from oscilloscope traces and plotting $\ln(A_t - A_\infty)$ *versus* time. These plots were linear ($r^2 > 0.997$) for at least 2 half-lives of reaction. A sample plot for the reaction between $Re_2(CO)_{10}$ and $NOBF_4$ is shown in Fig. 1. Absorbance changes of the reactant solution were checked with the Perkin-Elmer 330 spectrophotometer before and after each kinetic run. Usually the calculated and observed values agreed. Reproducibilities of rate constants were determined to be ±30%. Errors were large because of inaccuracies in determining A_∞ and the limitations of the stopped-flow spectrometer for handling extremely air-sensitive solutions (especially $NOBF_4$). Acceptable results can be obtained by using the same reactant solutions and performing all kinetic experiments on the same day.

For UV monitored experiments with $Cu(O_3SCF_3)_2$ in CH_3CN, a solution of $Cu(O_3SCF_3)_2$ was prepared in the cell, and an initial absorbance value was measured. An intense metal to ligand charge transfer band lies in the UV region where the carbonyl complexes absorb. The intensity of the Cu^{2+} derived transition is greater with an increase in temperature or in the presence of electrolyte. It was essential to

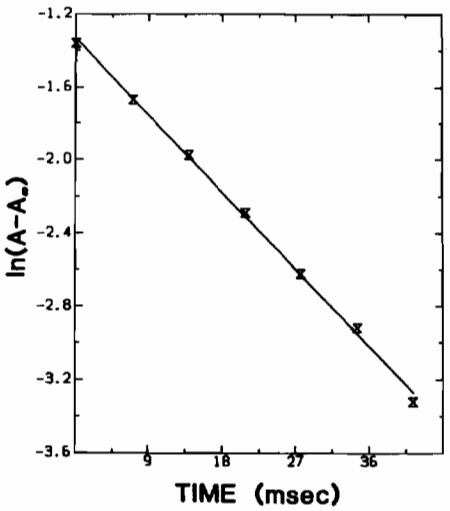

Fig. 1. Plot of $\ln(A_t - A_\infty)$ for the reaction between $Re_2(CO)_{10}$ (6.22×10^{-4} M) and $NOBF_4$ (1.24×10^{-2} M) in CH_3CN solvent at 22 °C as determined by stopped-flow methods.

let the solution equilibrate so a constant value of A_0 can be measured before beginning a kinetics run. Temperature control (±0.2 °C) was provided by a Haake circulating bath connected to the cell holder of the UV–Vis spectrometers. A solution of complex was injected into the cell, which was shaken vigorously. The decrease of complex was followed for at least 3 half-lives. An IR sampling technique was employed for a kinetic measurement with $Mn_2(CO)_{10}$ and $Cu(O_3SCF_3)_2$, and there was good agreement between this rate and the spectrophotometric value. All rate constants were measured under pseudo-first order conditions with $[Cu(O_3SCF_3)_2]$ at least 70 times that of the carbonyl complex. Plots of $\ln(A_t - A_\infty)$ *versus* time were linear ($r^2 > 0.995$) for 2–3 half-lives of reaction. Linear least-squares analysis provided rate constants and errors for all kinetic data (errors reported are one standard deviation).

Preparations

When necessary, manipulations were carried out under an atmosphere of prepurified nitrogen using standard Schlenk and syringe techniques. Air-sensitive solids were handled and stored in a Vacuum Atmospheres glove box equipped with an HE-493 dri train. A high vacuum line was used to remove water from hygroscopic metal salts, and $SnCl_4$ was purified by trap-to-trap distillation. The compounds $[Fe(phen)_3][ClO_4]_3$ [15], $[Cp_2Fe][BF_4]$ [16], $[Ru(bipy)_2Cl_2]PF_6$ [5], [PPN][O_3SCF_3] [17], $MnRe(CO)_{10}$ [18], and $[C_7H_7]BF_4$ [19] were prepared and characterized by published procedures.

Anhydrous Metal Salts ($CuCl_2$, $FeCl_3$) [20]

Thionyl chloride was freshly distilled before use. The hydrated metal salt (10 g $FeCl_3 \cdot 6H_2O$ or $CuCl_2 \cdot 2H_2O$) was pulverized by mortar and pestle and transferred to a 50 ml Schlenk flask. Thionyl chloride was added (25 ml) after several pump–purge cycles. For $FeCl_3 \cdot 6H_2O$ gas evolution occurs immediately; for $CuCl_2 \cdot 2H_2O$ no reaction occurs at room temperature. After gas evolution ceases, the $SOCl_2$ is refluxed for 1½ h and then removed by distillation. The last traces of $SOCl_2$ were removed at 25 °C under dynamic vacuum. Total yield of anhydrous salt is 70%.

$Cu(O_3SCF_3)_2$

Following the reaction reported by Dines [21] $Cu_2(OH)_2CO_3$ (1.41 g, 6.4 mmol) was placed in a 50 ml Schlenk flask and 5 ml of H_2O was added. Triflic acid (2.5 ml, 28 mmol) was dissolved in 4 ml of distilled H_2O. After cooling, the acid solution was added drop by drop to the copper solution. Immediate gas evolution occurs with the clear, blue solution turning dark brown. The solution was stirred for 10 min and a deep blue solution results. The solution is filtered and the volatile components are removed on a Schlenk line at 60 °C. The solid was placed on a high vacuum line and the pale blue solid was heated to 100 °C for 3 h. Recrystallization from hot anhydrous ethanol produced the title complex as a white powder in 90% yield.

Reaction of $M_2(CO)_{10}$ ($M_2 = Mn_2$, Re_2) with Oxidants

In a typical experiment the decacarbonyl (0.06 mmol) was added to 10 ml of CH_3CN. The oxidant (0.26 mmol, 2 equivalents) was added under a stream of N_2 and stirred until dissolved. Progress of the reaction was determined by IR spectroscopy.

Results

Oxidation of the metal–metal bond of $M_2(CO)_{10}$ complexes in CH_3CN solvent occurs for few of the oxidants investigated (Table I). These reactions were performed using at least two equivalents of oxidant according to eqn. (7).

$$M_2(CO)_{10} + 2Ox + 2CH_3CN \longrightarrow 2[M(CO)_5(NCCH_3)]^+ + 2Red \quad (7)$$

$M_2 = Mn_2, Re_2$

If no reaction occurred at room temperature the solution was heated to 50 °C for several hours and examined. Results are collected in Table I along with redox potentials of the oxidants. It was assumed that

TABLE I. Summary of Results from the Reaction Between $M_2(CO)_{10}$ (M = Mn, Re) and Oxidants in CH_3CN Solvent

Oxidant	Result	$E_{1/2}^{red}$ (V)[c]	Echem solvent/reference	Literature
$CuCl_2$	[a]	+0.85	PhCN/SCE	27a
$Cu(O_3SCF_3)_2$	[b]	+0.8	CH_3CN/SCE	27a
$NOBF_4$	[b]	1.22	CH_3CN/SCE	27b
$FeCl_3$	[a]			
$[Fe(phen)_3][ClO_4]_3$	[b]	+0.997	CH_3CN/SCE	27c
$AgBF_4$	N.R.	+0.27	CH_3CN/SCE	27d
$[Ru(bipy)_2Cl_2]PF_6$	N.R.	+0.32	CH_3CN/SCE	27e
$[Cp_2Fe]BF_4$	N.R.	+0.33	CH_3CN/SCE	27c
$[C_7H_7]BF_4$	N.R.	+0.06	CH_2Cl_2/SCE	27c
$Na_2[IrCl_6]\cdot 6H_2O$	N.R.	+0.40	H_2O/SCE	27c
$K_3[Fe(CN)_6]$	N.R.	−0.42	CH_3CN/Cr(biphenyl)$_2^+$	27c
$SnCl_4$	N.R.	+0.30	CH_3CN/SCE	27f
TCNE	N.R.	−0.17	CH_3CN/Ag-$AgClO_4$	27g
$Tl(O_2CCF_3)_3$	N.R.			

[a]Reaction occurs with production of $M(CO)_5Cl$ and $[M(CO)_5(NCCH_3)]^+$. [b]Reaction occurs with production of $[M(CO)_5(NCCH_3)]^+$. [c]Reduction potential of oxidant.

if $Mn_2(CO)_{10}$ did not react, then neither would the other dimetal decacarbonyls.

For $CuCl_2$ and $FeCl_3$, a mixture of products were obtained from their reactions with $M_2(CO)_{10}$. Simultaneous formation of $M(CO)_5Cl$ and $[M(CO)_5(NCCH_3)]^+$ occurs with slow conversion of $M(CO)_5Cl$ to the latter cation. Superposition of carbonyl peaks from each species complicated monitoring these reactions by IR. Also, in the UV–Vis spectrum, the absorptions from $[CuCl_4]^{2-}$, $[CuCl_3]^-$, $CuCl_2$, and $[CuCl]^+$ overlap in the spectrum. We do not know which Cu species is responsible for the $CuCl_2$ oxidation. When a sample of $CuCl_2$ is dissolved in CH_3CN, the following series of equilibria are rapidly established (eqn. (8)) [22].

$$Cu^{2+} \xrightarrow{Cl^-} [CuCl]^+ \xrightarrow{Cl^-} CuCl_2 \xrightarrow{Cl^-} [CuCl_3]^- \xrightarrow{Cl^-} [CuCl_4]^{2-} \quad (8)$$

A solution of $[CuCl_4]^{2-}$ was prepared by dissolving $CuCl_2$ in CH_3CN and adding $[NEt_4][Cl]$ until the electronic spectrum exhibits absorptions characteristic of this species. This solution would not oxidize $Mn_2(CO)_{10}$.

The reaction between $M_2(CO)_{10}$ and $[Fe(phen)_3][ClO_4]_3$ occurred rapidly. An approximate rate constant was measured with a pseudo-first order excess of $[Fe(phen)_3][ClO_4]_3$ (5.84×10^{-4} M) and $[Re_2(CO)_{10}] = 2.92 \times 10^{-5}$ M. Formation of $[Fe(phen)_3]^{2+}$ was monitored at 449 nm and a k_{obs} of 3×10^{-1} s^{-1} was obtained at 21 °C.

With $NOBF_4$, the expected stoichiometry of eqn. (4) was confirmed by IR analysis. In a separate experiment it was shown that no reaction occurs between $Mn_2(CO)_{10}$ and NO in CH_3CN. Reactions were monitored by observing the decrease in absorbance of the $\sigma \rightarrow \sigma^*$ transition of the $M_2(CO)_{10}$ complexes as a function of time. Although individual kinetic runs are well behaved (Fig. 1) reproducibility using different solutions at different times is poor. This probably results from the extreme sensitivity of solutions of $[NO]^+$. Consistent results could be obtained by measuring the concentration and temperature dependencies of rate constants on the same day with the same reactant solutions. The reproducibility of rate constants under these conditions was about ±30%.

Complete listings of pseudo-first order rate constants for the reactions with $NOBF_4$ are given in Table II. For each rate constant measurement linear plots of $\ln(A_t - A_\infty)$ *versus* t were obtained (Fig. 1). The dependence of k_{obs} on $NOBF_4$ concentration is illustrated graphically in Fig. 2, which establishes a linear dependence on the concentration of $NOBF_4$ ($k = 3.3 \pm 0.2 \times 10^3$ s^{-1} M^{-1}). An approximate zero intercept is observed consistent with a second order reaction with no $NOBF_4$ independent pathway. Second order rate constants are listed in Table II. The dependence of temperature on k_2 yields crude activation parameters: $\Delta H^{\neq} = 6.3 \pm 1.3$ kcal mol^{-1} and $\Delta S^{\neq} = -24 \pm 5$ cal mol^{-1} K^{-1}.

Competition experiments were performed with 1:1 mixtures of $Mn_2(CO)_{10}$ and $Re_2(CO)_{10}$ (1.26×10^{-2} M in each) added to a deficiency of $NOBF_4$ (2.52×10^{-3} M). For pseudo-first order excesses of $M_2(CO)_{10}$, taking the ratio of pseudo-first order rate laws and integrating from time zero to infinity yields eqn. (9).

$$\frac{[Mn_2(CO)_{10}]_{lost}}{[Re_2(CO)_{10}]_{lost}} = \frac{k_{Mn}[Mn_2(CO)_{10}]}{k_{Re}[Re_2(CO)_{10}]} \quad (9)$$

TABLE II. Observed Rate Constants for eqn. (3) at 25 °C in CH_3CN

$M_2(CO)_{10}$	$[M_2(CO)_{10}] \times 10^5$ (M)	$[NOBF_4] \times 10^2$ (M)	k_{obs} [a] (s^{-1})	T (°C)	$k_2 \times 10^3$ ($s^{-1}\ M^{-1}$)
Mn_2 [b]	11.0	1.10	20.2[c]	21.0	1.84
	11.4	2.86	38.2	21.0	1.34
	12.1	4.28	32.6	21.0	0.76
Re_2 [d]	6.22	1.54	23.2[c]	21.0	1.51
	6.45	3.25	27.1[c]	21.0	0.83
	6.22	1.24	27.6[c]	21.0	2.23
	6.30	1.47	22.4[c]	21.0	1.52
	6.13	0.600	14.8	21.5	2.47
	6.13	1.24	33.7	21.5	2.72
	6.13	1.44	46.7	21.5	3.24
	6.13	3.20	100	21.5	3.13
	6.29	0.987	2.99	3.0	0.30
	6.29	0.987	4.81	14.0	0.49
	6.29	0.987	5.73	24.5	0.58
	6.29	0.987	11.4	34.0	1.16

[a]Rate constants are the average of 2 determinations. [b]Monitoring the rate of disappearance of $Mn_2(CO)_{10}$ at 342 nm. [c]Rate constants are the average of 4 separate runs. [d]Monitoring the rate of disappearance of $Re_2(CO)_{10}$ at 313 nm.

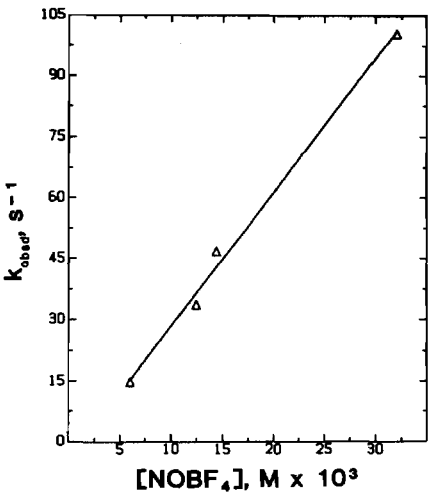

Fig. 2. Plots of k_{obs} (s^{-1}) *vs.* $NOBF_4$ concentration (M) for the reaction between $Re_2(CO)_{10}$ and $NOBF_4$ at 22 °C in CH_3CN.

The quantities of $[M_2(CO)_{10}]_{lost}$ ($M_2 = Mn_2, Re_2$) can be calculated in moles or concentration units. Three separate experiments were performed and analyzed by FTIR for the disappearance of $M_2(CO)_{10}$ to yield $k_{Mn}/k_{Re} = 3.0 \pm 0.7$.

Kinetics of the oxidation reaction between $Cu(O_3SCF_3)_2$ and $M_2(CO)_{10}$ ($M_2 = Mn_2$, MnRe, Re_2, eqn. (10)), can be followed by UV–Vis and IR spectroscopy (Fig. 3) as described in the experimental section.

$$M_2(CO)_{10} + 2Cu(O_3SCF_3)_2 \longrightarrow 2M(CO)_5(NCCH_3)^+ + 2Cu(O_3SCF_3) \quad (10)$$

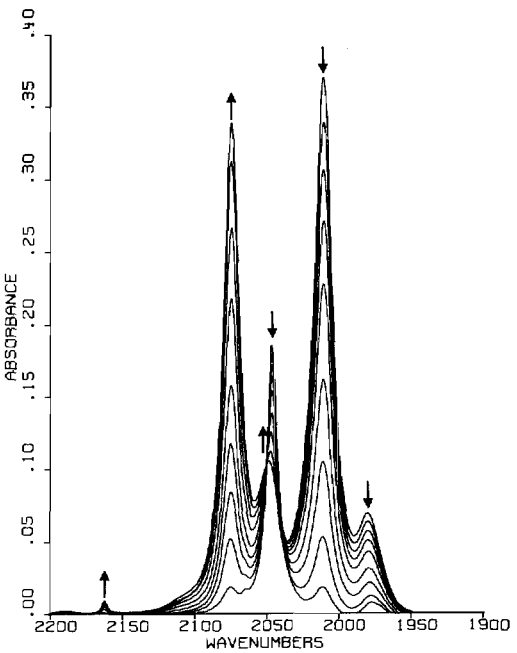

Fig. 3. Infrared spectral changes for the reaction between $Cu(O_3SCF_3)_2$ and $Mn_2(CO)_{10}$ in CH_3CN solvent.

Using a pseudo-first order excess of $Cu(O_3SCF_3)_2$ gave linear plots of $\ln(A_t - A_\infty)$ *versus* t for the rate of disappearance of $M_2(CO)_{10}$. The dependence of k_{obs} against the concentration of $Cu(O_3SCF_3)_2$, (Fig. 4) shows a second order rate law (eqn. (11))

$$\frac{-d[M_2(CO)_{10}]}{dt} = k_2[M_2(CO)_{10}][Cu(O_3SCF_3)_2] \quad (11)$$

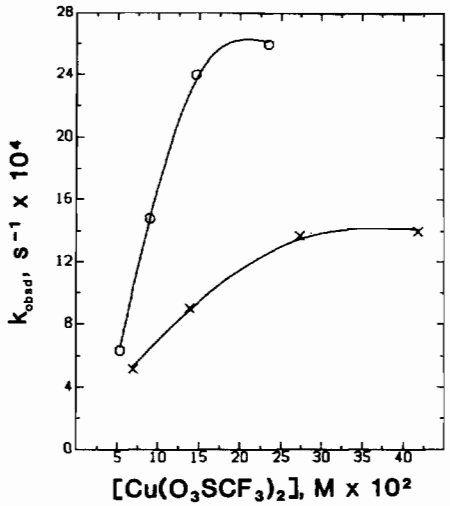

Fig. 4. Plot of k_{obs} (s^{-1}) *vs.* $Cu(O_3SCF_3)_2$ concentration for the reaction between $M_2(CO)_{10}$ and $Cu(O_3SCF_3)_2$ in CH_3CN; O = MnRe at 42.7 °C; X = Mn_2 at 48.5 °C.

at concentrations of $Cu(O_3SCF_3)_2$ below 1.40×10^{-2} M with attainment of a limiting rate at higher concentrations. Comparison of the second order rate constants among $M_2(CO)_{10}$ complexes and the determination of activation parameters were done at low [$Cu(O_3SCF_3)_2$]. Observed rate constants are summarized in Table III. Second order rate constants calculated for the three metal complexes at the same $Cu(O_3SCF_3)_2$ concentration and temperature are listed in Table IV along with activation parameters. Effects of ionic strength on observed rate constants were investigated using [n-Bu_4N][BF_4] as the electrolyte. Comparison of the observed rate constants with (0.034 M) and without added electrolyte shows no appreciable rate difference.

The dependence of reaction rates on [$Mn_2(CO)_{10}$] was studied at a constant ionic strength of 0.034 M [n-Bu_4N][BF_4] and 6.94×10^{-3} M $Cu(O_3SCF_3)_2$. The observed rate constants (Table V) suggest inhibition by increasing [$Mn_2(CO)_{10}$]. Inhibition also occurs with added triflate. A study of the triflate dependence was performed at a constant ionic strength of 0.448 M with varying amounts of $[BF_4]^-$ and $[CF_3SO_3]^-$ (Table V, Fig. 5). Absorptions in the electronic spectrum characteristic of $[Cu(O_3SCF_3)_4]^{2-}$ grow in with increasing $[CF_3SO_3^-]$ as the rate of reaction decreases.

Discussion

Oxidants that fail to react with $M_2(CO)_{10}$ compounds fall into two classes. First, $[Fe(CN)_6]^{3-}$ and $[IrCl_6]^{2-}$ may not react because they are anions. Although these oxidants are classified as strong on a thermodynamic basis there may be a high electrostatic barrier to outer sphere electron transfer to these complexes in aprotic solvents because of their high

TABLE III. Observed Rate Constants as a Function of Temperature and Concentration for the Reaction Between $M_2(CO)_{10}$ (M_2 = Mn_2, MnRe, Re_2) and $Cu(O_3SCF_3)_2$ in CH_3CN

M_2	T (°C)	[$M_2(CO)_{10}$] x 10^5 (M)	[$Cu(O_3SCF_3)_2$] x 10^3 (M)	k_{obs} x 10^4 (s^{-1})
Mn_2[a]	48.5	7.65	6.95	5.15
	48.5	8.18	13.8	9.00
	48.5	7.58	27.3	13.7
	48.4	6.29	41.7	14.0
	38.0	9.35	27.6	6.27
	56.7	9.35	27.6	15.1
	56.0	9.35	27.6	31.2
	68.3	9.35	27.6	95.3
	34.8	110	12.2	2.39[b]
MnRe[c]	42.7	7.49	5.27	6.35
	42.7	7.29	8.98	14.8
	42.7	7.10	14.6	24.0
	42.7	6.64	23.5	26.0
	31.2	8.45	11.9	6.65
	38.6	8.45	11.9	12.1
	47.2	8.45	11.9	20.5
	56.2	8.45	11.9	60.6
Re_2[d]	45.0	6.45	7.50	4.98
	49.1	8.13	7.42	12.4

[a]Monitoring the rate of disappearance of $Mn_2(CO)_{10}$ at 342 nm. [b]Monitoring the rate of disappearance of $Mn_2(CO)_{10}$ at 2011 cm^{-1}. [c]Monitoring the rate of disappearance of $MnRe(CO)_{10}$ at 323 nm. [d]Monitoring the rate of disappearance of $Re_2(CO)_{10}$ at 313 nm.

TABLE IV. Second Order Rate Constants and Activation Parameters for the Reaction Between $M_2(CO)_{10}$ (M_2 = Mn_2, MnRe, Re_2) and $Cu(O_3SCF_3)_2$ in CH_3CN

$M_2(CO)_{10}$	k_2 (s^{-1} M^{-1})	$\Delta H^{\neq}$ (kcal mol^{-1})	$\Delta S^{\neq}$ (cal mol^{-1} K^{-1})
Mn	6.4×10^{-2} [a]	18.0 ± 0.5[b]	−8.0 ± 1.7
MnRe	2.6×10^{-1} [a]	16.0 ± 2.0	−11.0 ± 6.0
Re_2	1.7×10^{-1}	–	–

[a]Calculated at 49.1 °C at $[Cu(O_3SCF_3)_2] = 7.42 \times 10^{-3}$ M using experimental activation parameters. [b]Errors represent one standard deviation from a least-squares analysis.

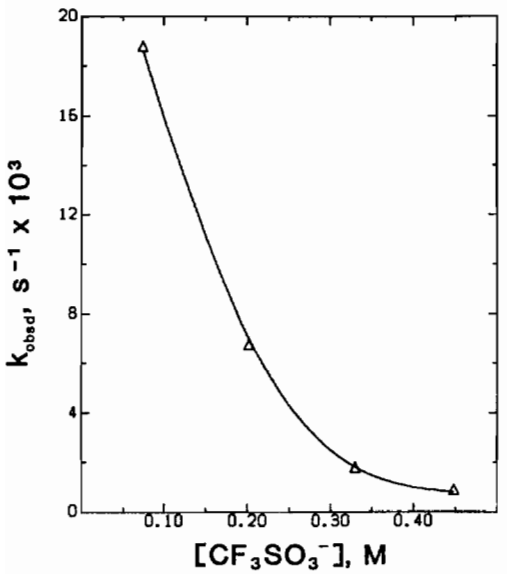

Fig. 5. Plot of k_{obs} (s^{-1}) *vs.* $[CF_3SO_3^-]$ (M) for the reaction of $Mn_2(CO)_{10}$ and $Cu(O_3SCF_3)_2$ at constant ionic strength in CH_3CN.

negative charge. Second, cationic oxidants that do not react have low values of $E_{1/2}$ (Table I) and may not be able to oxidize $M_2(CO)_{10}$ because of thermodynamic constraints.

A reported reaction between $Mn_2(CO)_{10}$ and TCNE in THF[11] was found not to occur in CH_3CN. This may result from a less favorable redox potential in CH_3CN or from the occurrence of only a minor amount of reaction that was detected in the EPR work in THF solvent, but would not be detectable by IR in our experiments.

Compounds that oxidize $M_2(CO)_{10}$ (M_2 = Mn_2, Re_2) in CH_3CN are all cationic or neutral. Furthermore, $[Fe(phen)_3]^{3+}$, $[NO]^+$, and $Cu(O_3SCF_3)_2$ are strong oxidants in CH_3CN solvent. The rates of reaction of these oxidants with $M_2(CO)_{10}$ complexes follows the order $NO^+ \gg Fe(phen)_3^{3+} > Cu(O_3SCF_3)_2$, which parallels their oxidizing ability. Two of these species have been classified as outer sphere oxidants, $[Fe(phen)_3]^{3+}$ [15] and $Cu(O_3SCF_3)_2$ [23]. Another class of oxidants, anhydrous metal chlorides, exist as mixtures of chlorometal complexes e.g., in CH_3CN solution (e.g. eqn. (8)). Ligand deficient complexes, Cu^{2+} or $[CuCl]^+$ [22], appear to be the active oxidants in the reactions we studied.

Kinetic studies of the reaction between $NOBF_4$ and $M_2(CO)_{10}$ (M_2 = Mn_2, Re_2) show a first order dependence on the carbonyl complex and on the concentration of $NOBF_4$, which suggests an associative mechanism. The small enthalpy of activation (6.3 kcal mol^{-1}) and large negative entropy of activation (−24 cal mol^{-1} K^{-1}) are typical of outer sphere electron transfer reactions [24]. For example, the oxidation of $[CpFe(CO)_2]_2$ by $[Ru(bipy)_2Cl_2][PF_6]$ in CH_3CN was reported [6] to be outer sphere and associative in nature with $\Delta H^{\neq} = 6.2 \pm -0.5$ kcal mol^{-1} and $\Delta S^{\neq} = -16.6 \pm 1.5$ cal mol^{-1} K^{-1}. Two proposed mechanisms for oxidation of $M_2(CO)_{10}$ (M_2 = Mn_2, Re_2) in CH_3CN are outlined in Scheme 1.

TABLE V. Effect of Concentration and Backing Electrolyte on Observed Rate Constants in the Reaction Between $Mn_2(CO)_{10}$ and $Cu(O_3SCF_3)_2$ at 48.0 °C in CH_3CN

$[Mn_2(CO)_{10}]$[a] x 10^5 (M)	$[Cu(O_3SCF_3)_2]$ x 10^3 (M)	$[n\text{-}Bu_4N][BF_4]$ (M)	$[PPN][O_3SCF_3]$ (M)	k_{obs} x 10^4 (s^{-1})
9.00	6.95	0.034		5.77
18.0	6.94	0.034		2.83
3.82	6.94	0.034		9.86
9.94	40.7		0.191	22.3
9.94	39.7	0.193		66.0
9.94	39.2		0.448	9.23
9.94	39.2	0.246	0.202	67.6
9.94	39.2	0.118	0.330	18.0
9.94	39.2	0.379	0.074	188

[a]Monitoring the rate disappearance of $Mn_2(CO)_{10}$ at 342 nm.

A

$$M_2(CO)_{10} + [NQ]^+ \xrightarrow{slow} [M_2(CO)_{10}]^+ + NO \quad (12)$$

$$[M_2(CO)_{10}]^+ \xrightarrow[CH_3CN]{fast} [M(CO)_5(NCCH_3)]^+ + M(CO)_5 \quad (13)$$

$$M(CO)_5 + [NO]^+ \xrightarrow[CH_3CN]{fast} [M(CO)_5(NCCH_3)]^+ + NO \quad (14)$$

B

$$M_2(CO)_{10} + NO^+ \xrightarrow{slow} M_2(CO)_{10}^+ + NO \quad (15)$$

$$[M_2(CO)_{10}]^+ + NO^+ \xrightarrow{fast} [M_2(CO)_{10}]^{2+} + NO \quad (16)$$

$$[M_2(CO)_{10}]^{2+} \xrightarrow{fast} 2[M(CO)_5(NCCH_3)]^+ \quad (17)$$

Scheme 1.

Attempts to observe radical intermediates (Scheme 1, pathway A, eqn. (13)), by performing the oxidation in the presence of CCl_4, to produce $Mn(CO)_5Cl$, failed. Irradiation [25] of $Mn_2(CO)_{10}$ in CH_2Cl_2/0.1 M $[n\text{-}Bu_4N][ClO_4]$ containing variable amounts of CCl_4 and $[Cp_2Fe]^+$ yields $Mn(CO)_5Cl$ and $Mn(CO)_5(ClO_4)$. The latter compound is obtained from oxidation of $[Mn(CO)_5]$ by $[Cp_2Fe]^+$ with ClO_4^- scavenging the 16-valence electron $[Mn(CO)_5]^+$. This suggests that oxidation of the radicals generated by cleavage of metal–metal bonds is a viable pathway even in the presence of a good halogen donor such as CCl_4. Furthermore, Hepp and Wrighton [25] found a correlation between the formal potential of the redox couple and the amount of oxidized product. Thus, one would expect to see $M(CO)_5Cl$ form in the presence of weak oxidants. Indeed with $FeCl_3$ and $CuCl_2$, some $M(CO)_5Cl$ was formed during the oxidation. Apparently, the $Mn(CO)_5$ radical formed from $[M_2(CO)_{10}]^+$ abstracts a chloride faster than the Fe or Cu complex can oxidize it to $[M(CO)_5]^+$. These observations tentatively favor mechanism A of Scheme 1.

Interaction of $Cu(O_3SCF_3)_2$ and $M_2(CO)_{10}$ (M_2 = Mn_2, MnRe, Re_2) in CH_3CN leads to oxidation. The reaction obeys the second order rate law given in eqn. (10) at low concentrations of $Cu(O_3SCF_3)_2$. In this concentration regime the first order dependence on $[Cu(O_3SCF_3)_2]$ suggests an associative mechanism operates and the negative entropies of activation (Table V) also agree with an associative reaction scheme. The decrease in the k_{obs} at high concentrations of $Mn_2(CO)_{12}$ cannot be explained at present.

There is an interesting difference between relative reactivities of the outer sphere oxidation processes characterized here and halogen oxidations of the $M_2(CO)_{10}$ complexes. The relative ease of oxidation of $Mn_2(CO)_{10}$, $MnRe(CO)_{10}$, and $Re_2(CO)_{10}$ by the outer sphere reagent NO^+ increases slightly along the series $Re_2 < MnRe < Mn_2$. However, for the reaction with $Cu(O_3SCF_3)_2$, another presumed outer sphere oxidant, the reactivity ordering is $MnRe \sim Re_2 > Mn_2$. Again the variation in reactivity is small. An electrochemical study [26] places the anodic waves at the same potential (1.56 V *versus* SCE) for all three dinuclear compounds in CH_3CN solvent. Similarity in redox potentials may account for the small spread in reactivity with outer sphere oxidants. For the halogen inner sphere oxidants a reactivity order $Mn_2 < MnRe < Re_2$ holds [11] and spans three orders of magnitude. This trend was attributed to the greater importance of steric accessibility to the metal–metal bond, that is greatest in the dirhenium system. It will be interesting to see the kinds of periodic trends found in other cluster systems.

Acknowledgements

This material is based on work supported by the National Science Foundation under Grants No. CHE82-10514 (F.B.) and No. CHE85-4088 (W.C.T.). W.C.T. thanks the Alfred P. Sloan Foundation for a research fellowship.

References

1 W. E. Geiger and N. G. Connelly, *Adv. Organomet. Chem., 24,* 87 (1985).
2 J. A. Ferguson and T. J. Meyer, *J. Am. Chem. Soc., 94,* 3409 (1972).
3 J. H. Espenson, *Inorg. Chem., 7,* 631 (1968).
4 J. H. Espenson and D. J. Boone, *Inorg. Chem., 7,* 636 (1968).
5 J. H. Espenson and R. J. Kinney, *Inorg. Chem., 10,* 376 (1971).
6 J. N. Braddock and T. J. Meyer, *Inorg. Chem., 12,* 723 (1973).
7 N. G. Connelly and L. F. Dahl, *J. Chem. Soc., Chem. Commun.,* 880 (1970).
8 D. Drew and D. J. Darensbourg, M. Y. Darensbourg, *Inorg. Chem., 14,* 1579 (1975).
9 N. G. Connelly and J. D. Davies, *J. Organomet. Chem., 38,* 385 (1972).
10 P. J. Krusic, H. Stoklosa, L. E. Manzer and P. Meakin, *J. Am. Chem. Soc., 97,* 667 (1975).
11 S. P. Schmidt, W. C. Trogler and F. Basolo, *J. Am. Chem. Soc., 106,* 1308 (1984).
12 H. Taube, 'Electron Transfer Reactions of Complex Ions in Solution', Academic Press, New York, 1970.
13 G. R. John, B. F. G. Johnson, J. Lewis and A. L. Mann, *J. Organomet. Chem., 171,* C9 (1979).
14 M. Windholz (ed.), 'The Merck Index – An Encyclopedia

of Chemicals, Drugs and Biologicals', 10th edn., Merck, N.J., 1983, p. 6498.
15 F. P. Dwyer and H. A. McKenzie, *J. Proc. R. Soc. N.S.W., 81*, 93 (1947).
16 D. N. Hendrickson, Y. S. Sohn and H. B. Gray, *Inorg. Chem., 10*, 1559 (1971).
17 J. Nitschke, S. P. Schmidt and W. C. Trogler, *Inorg. Chem., 24*, 1972 (1985).
18 S. P. Schmidt, F. Basolo, C. M. Jensen and W. C. Trogler, *J. Am. Chem. Soc., 108*, 1894 (1986).
19 K. Conrow, *Org. Synth., 5*, 1138 (1973).
20 A. R. Pray, *Inorg. Synth., 5*, 153 (1952).
21 M. B. Dines, *J. Inorg. Nucl. Chem., 38*, 1380 (1976).
22 C. L. Jenkins and J. K. Kochi, *J. Am. Chem. Soc., 94*, 856 (1972).
23 C. L. Jenkins and J. K. Kochi, *J. Am. Chem. Soc., 94*, 843 (1972).
24 F. Basolo and R. G. Pearson, 'Mechanisms of Inorganic Reactions', 2nd edn., Wiley, New York, 1967.
25 A. F. Hepp and M. S. Wrighton, *J. Am. Chem. Soc., 103*, 1258 (1981).
26 C. J. Pickett and D. Pletcher, *J. Chem. Soc., Dalton Trans.*, 879 (1975).
27 (a) P. Zuman, A. Narayanan, T. L. Fenner, J. Jandik and G. A. Shia, 'Handbook Series in Inorganic Electrochemistry', Vol. 2, CRC Press, Boca Raton, Fl., 1981; (b) Vol. 4, 1984; (c) Vol. 3, 1983; (d) Vol. 1, 1980; (e) Vol. 6, 1986; (f) Vol. 8, 1986; (g) P. H. Rieger, I. Bernal, W. Reinmuth and G. K. Frankel, *J. Am. Chem. Soc., 85*, 683 (1963).